

## Stress profiles at contact surface in ring compression test<sup>†</sup>

Jeong Hoon Noh, Min Tae Kim and Beong Bok Hwang\*

*Department of Mechanical Engineering, Inha University, 253 Yonghyun-dong Nam-gu, Incheon, Korea*

(Manuscript Received June 25, 2009; Revised March 15, 2010; Accepted March 22, 2010)

### Abstract

A perfectly plastic material has been employed as a model material in simulation to analyze numerically the ring compression process, especially to examine the deformation patterns along the die/workpiece interface, which is strongly related to the frictional condition at the contact boundary. The main objective is to provide the deformation characteristics in detail in ring compression, especially at the tool/workpiece interface. The surface flow patterns at the contact boundary in ring compression are summarized and analyzed in terms of surface expansion, surface expansion velocity, pressure distributions exerted on the die surface, relative sliding velocity between die and workpiece, and sliding distance along the die surface. Movement of neutral positions and folding phenomenon are also investigated to see the effect on the deformation patterns at the interface, that is, geometrical change, which is important to measure the frictional condition at the interface using calibration curves. Finite element (FE) simulation using rigid-plastic finite element code has been performed for analysis. The results of this study reveal that surface expansion as well as other surface flow patterns, such as sliding velocity and so on, shows different and distinctive characteristics between low and high frictional conditions at the interface. This is directly related to the movement of neutral positions and folding, which affects the sensitivity of dimensional changes to tribological conditions at the interface.

*Keywords:* Ring compression test; Surface expansion; Sliding velocity; Sensitivity; Folding; Neutral position

### 1. Introduction

In ring compression, the internal diameter in the middle section of the specimen may increase, decrease or remain constant, depending on the amount of frictional retardation stresses imposed by tools and the lubricants at the tool/workpiece interface [1]. Due to the sensitive change in internal diameter of the compressed ring to interfacial friction, the ring compression test has been widely used to evaluate the friction condition in metal forming processes [2]. When evaluating these tests, the tribological condition at the interface of the ring specimen does not remain the same throughout the tests. Furthermore, interfacial friction has a significant effect on material deformation, forming load, component surface finish and tool wear and also an essential input parameter for FE analysis in forming process design and production [3].

In analysis of metal forming processes, Coulomb's law or Amonton's law of friction [4-6] and constant shear friction law [7-9] have traditionally been assumed to simulate forming processes. The frictional stress is proportional to the normal stress,  $\tau = \mu P$ , in the Coulomb friction law, while the frictional

stress is a certain fraction of shear yield stress of workpiece material,  $\mu = mk$ , in constant shear friction law. Since frictional stress depends on the normal stress, the Coulomb friction law seems to describe the real behavior of friction better than the constant shear friction. However, the constant shear friction law is widely used in simulation of bulk metal forming processes due to its theoretical simplicity and numerical rigidity. In reality, the two laws give nearly the same results for ring compression since the normal stress distribution in this case is relatively uniform. However, for complex forming processes, such as backward extrusion in which the normal stress may vary widely across the tool-workpiece interface, the two friction laws may give quite different results [10].

In the present study, the ring compression test has been numerically analyzed in order to investigate the deformation characteristics at the tool/workpiece interface in detail. The constant shear friction is assumed as a single parameter in order to see the effect of friction factor on the surface deformation patterns. Surface expansion and normal pressure distributions along the tool/workpiece interface are predicted under selected frictional condition for qualitative analysis of the lubricant conditions. Relative sliding velocity distribution is also calculated at the contact boundary, which is considered as one of important parameters for evaluation of hydrodynamic lubrication together with normal pressure distribution.

<sup>†</sup>This paper was recommended for publication in revised form by Associate Editor

In-Ha Sung

\*Corresponding author. Tel.: +82 32 860 7387, Fax: +82 32 868 1716

E-mail address: bbhwang@inha.ac.kr

© KSME & Springer 2010

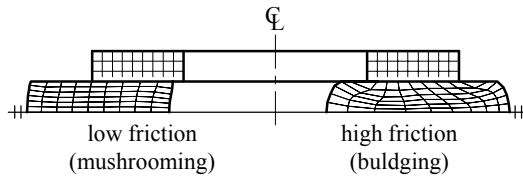


Fig. 1. Effect of friction on metal flow in ring compression test.

- $D_0$  : Initial billet outer diameter
- $d_0$  : Initial billet inner diameter
- $H$  : Initial billet height
- $D_1$  : Final billet outer diameter
- $d_1$  : Final billet inner diameter
- $h$  : Final billet height
- $h_{st}$  : Stroke (50% of height)
- $\square$  : Material points on die surface
- $\circ$  : Material points on billet surface
- $\oplus$  : Folded point

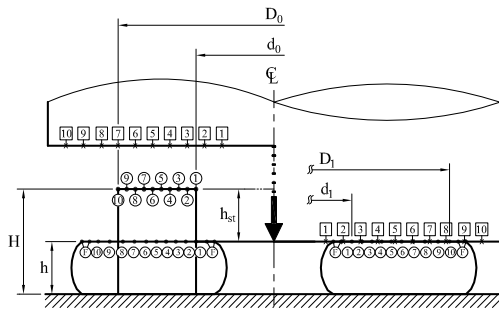


Fig. 2. Material points used as an abscissa in analysis.

Predictions are also made in terms of sliding distance of the material on the die surface, which is essential to the assessment of the wear behavior of tools. Due to the advantages of there being no need of force measurement during the test, or the knowledge of the flow stress of the material, this method has been widely used in metal forming [11]. A perfectly plastic and rate-insensitive material was employed as a model material for simulations such as the yield strength  $Y = 100$  MPa. A commercially available FEM tool, Deform2-DTM [12], has been used for numerical analysis, which is programmed in rigid plasticity theory [13].

## 2. Method of analysis

In a ring compression test, the internal diameter of the ring at the middle section increases when the friction factor is low, while increasing friction results in an outward flow of the material as schematically shown in Fig. 1. The method uses the finite element technique with assumed friction value prescribed and includes fitting or calibration curves to the experimental data for evaluating a current friction value based on measured changes of the ring dimensions.

To investigate the deformation characteristics of the ring compression process and then determine the frictional calibration curves of the model material, i.e., a perfectly plastic material, Deform2-DTM finite element code was used in the simulation of simple compression of a cylindrical ring, 50.8 mm in outer diameter, 25.4 mm in internal diameter, and 16.9 mm in height, which is known as a ‘standard’ specimen. Due to the nature of symmetry, one quarter of the ring specimen was represented to construct a 2-D model. A total of 2000 quadri-

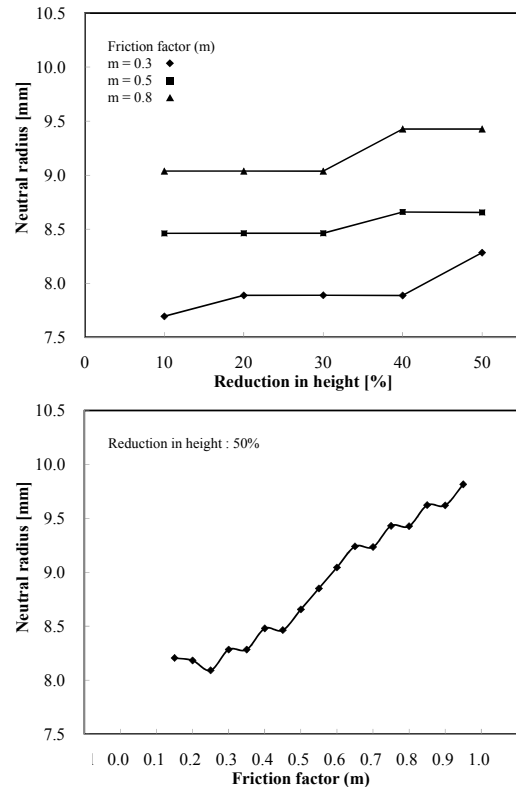


Fig. 3. Locations of neutral position as functions of reduction in height (top) and friction factor (bottom).

lateral elements were employed to model the specimen. The top and bottom platens were modeled as a rigid body. The die velocity was kept constant at 1.0 mm/sec., and the simulation was performed over the whole range of friction factor from 0.0 to 1.0, that is, from frictionless to sticking condition. The compression process ended when the reduction in height reached at 50%, for which 100 to 150 time steps were required. In Fig. 2, the geometry of the test specimen before and after deformation is schematically illustrated. Figure 2 also depicts the material points on the surface of die and workpiece used for horizontal coordinate as an abscissa in figures in the present study.

## 3. Results of analysis

### 3.1 Neutral positions and folding

Movement of the neutral radius in the ring compression test is shown in Fig. 3 as a function of the reduction in height (top) and as a function of the friction factor (bottom), respectively. It is revealed in the figure that the location of the neutral position for higher friction tends to remain constant until the reduction in height reaches 30% and then moves outwards. After 30% reduction in height, the neutral radius increases abruptly and then remains constant. This trend is amplified with increasing the friction factor. For relatively low friction, the location of the neutral position moves outward in the beginning of the process, remains constant, and finally expands

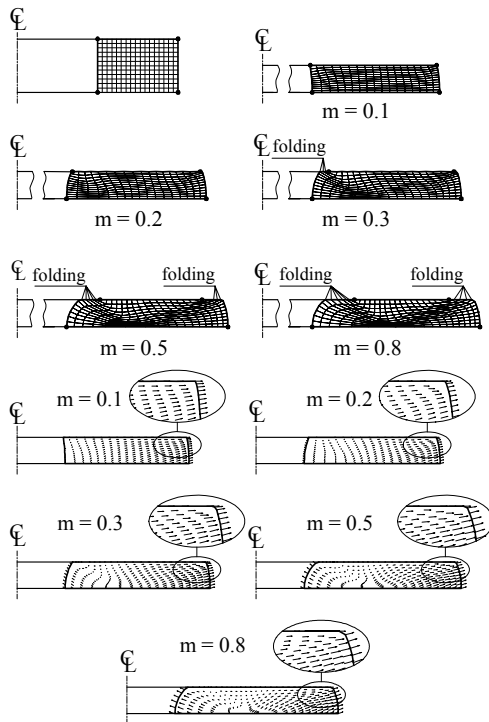


Fig. 4. Mesh distortions (top) and relative nodal velocity distributions (bottom) at 50% reduction in height for various friction factors.

outward near the end of the process. Note that under low frictional conditions, i.e., below 0.2 of the friction factor, at the contact boundary the neutral radius vanishes and the internal diameter increases as the deformation proceeds.

At the final stage of the process for different frictional conditions, at 50% reduction in height, the neutral radius is described as a function of the friction factor in the figure (bottom), in which it is seen that the neutral radius increases almost linearly as the friction factor increases. It can be also seen in the figure that the interfacial friction is proportional directly to the neutral radius and can therefore be estimated by measuring the changes of internal or outer diameter and using the calibration curves, which are usually plotted as friction factor versus reduction in ring height and decrease in internal diameter.

The deformation patterns of selected cases are shown in Fig. 4 in terms of mesh distortions (top) and relative nodal velocity distributions between die and workpiece (bottom). In the figure, it is easily seen that folding occurs more easily as the friction factor increases. Folding occurs at the inner surface as well as the outer surface for high friction. It is also revealed that the folding phenomenon is seen only for high friction, that is,  $m > 0.2$ , and is amplified with increasing friction factor. For  $m = 0.2$ , the internal diameter at the interface and at the middle of the specimen is almost the same, and both diameters at the middle and at the interface do not change during the process. However, the 'barreling' or the decrease in internal diameter at the middle of the specimen is more than that at the contact inter-face for friction factor greater than 0.2.

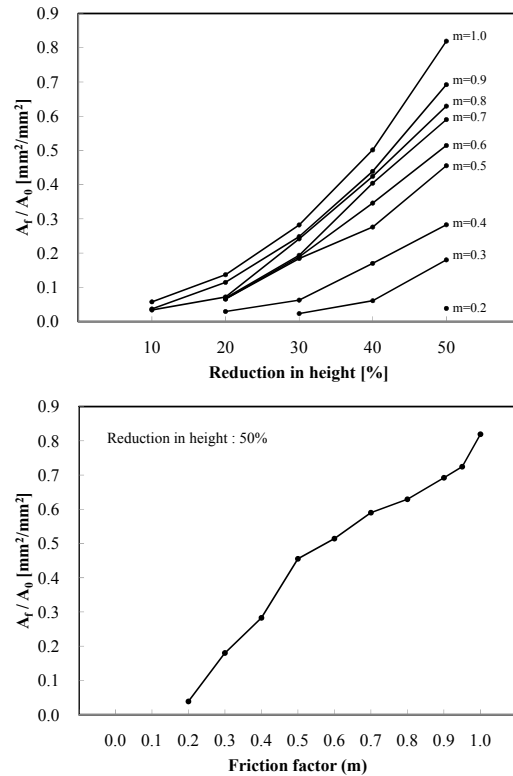


Fig. 5. Folded area as functions of reduction in height for various friction factors (top) and friction factors at 50% reduction in height (bottom).

It is also known easily from the figure that the relative velocity in the normal direction, i.e., upwards, on the lateral surface of the specimen increases with increasing friction, which leads to folding. It is easily noted that a unique boundary is defined with the magnitude of friction factor for  $m = 0.2$ . For friction factor less than 0.2, the neutral radius vanishes and 'mushrooming' phenomenon occurs. Note that the number of elements used is a total of 204 only in this case for clear view of velocity vectors in the figure and no remeshing is experienced even if a proper criterion is provided in the program under severe frictional condition. It should be also noted the ring compression process, during simulations with a Lagrangian mesh, does not have any difficulties in incorporating the die boundary shape into the FEM mesh with increasing relative displacement and in accommodating the considerable changes of deformation mode with the mesh system provided.

Fig. 5 shows the folded area as a function of reduction in height for various friction factors (top) and friction factors at 50% reduction in height (bottom), respectively. It is easily seen that folding just starts to occur for  $m = 0.2$  at 50% reduction in height. The folded area increases as the friction factor and reduction in height increase, and this trend is intensified with increasing friction factor. At sticking friction, the folded area is almost equal to the initial contact area at the end of the process. For a friction factor greater than 0.5, folding occurs in the beginning of the process and the folded area expands further throughout the process. It is also known in the figure that

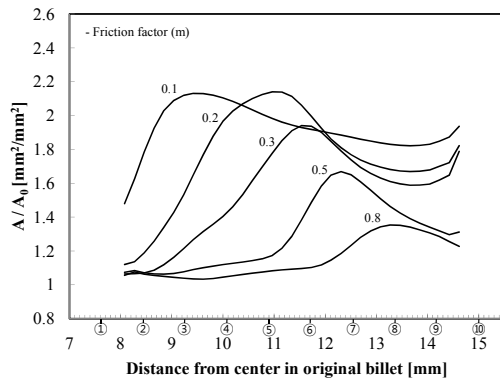


Fig. 6. Surface expansion for various friction factors.

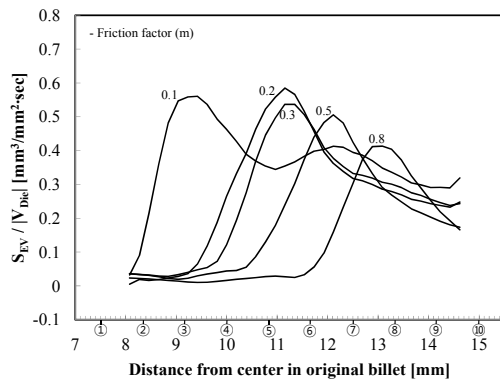


Fig. 7. Surface expansion velocity for various friction factors.

the folded area at the end of the process increases more sharply at low friction than at high friction.

### 3.2 Surface deformation patterns

Surface stresses have been predicted in terms of surface expansion, surface expansion velocity, contact pressure, relative velocity between die and workpiece, and sliding distance of workpiece on the die surface. These values constitute surface load profiles which describe the severity of surface deformation.

The relationship between surface expansion ( $A/A_0$ ) and the distance from the center in the original billet for various friction factors at 50% reduction in height is shown in Fig. 6. It is seen that the surface area of the workpiece increases more easily as the friction factor decreases, and the surface expansion increases sharply near the inner periphery of the workpiece at low friction. However, the location of maximum surface expansion moves outward and its peak value decreases as the friction factor increases. The surface area does not expand significantly over the whole surface except near the outer periphery at high friction. It is also noted in the figure that for friction factor  $m = 0.2$ , which is moderate frictional condition, the maximum surface expansion is almost the same as that for  $m = 0.1$ , while its location moves away from the center.

For medium friction, the greatest surface expansion occurs in the middle of the contact surface. Also, the surface expan-

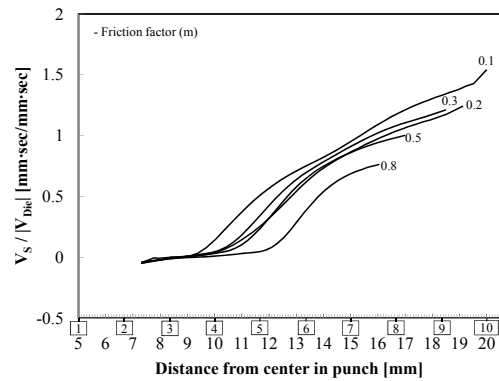


Fig. 8. Sliding velocity for various friction factors.

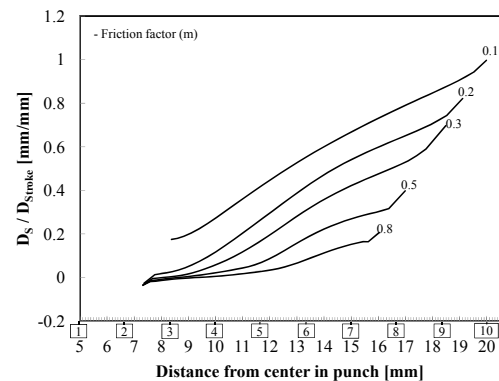


Fig. 9. Sliding distance for various friction factors.

sion is greatest at the region near the inner periphery at low friction and near the outer periphery at high friction, respectively.

It is interesting to see the surface expansion velocity ( $S_{EV}/|V_{Die}|$ ) normalized by the die speed at various positions on workpiece surface as shown in Fig. 7. As in Fig. 6, the surface expansion occurs widely over the whole contact surface at low friction except the region near the inner periphery. The location of maximum surface expansion velocity moves outward and its peak value decreases gradually as the friction factor increases, while the difference between peak values for various friction factors is not remarkable. The surface expansion velocity seems almost the same at the region near the outer periphery over the whole range of frictional condition.

Fig. 8 shows the relative sliding velocity ( $V_s/|V_{Die}|$ ) of workpiece on the die surface, which is also normalized by the die speed. It is easily known in the figure that the relative sliding movement increases as the location of die surface moves in the radial direction, and this trend is intensified with decreasing friction factor. The relative sliding movement near the center seems not so significant over all range of friction.

Sliding distances ( $D_s/D_{Stroke}$ ) of the workpiece on the particular location of the die surface are predicted and shown in Fig. 9, which is normalized by the punch stroke. Sliding distance together with sliding velocity and contact pressure is an important surface stress and can be used to measure tool life and/or failure in terms of wear. It is easily known in the figure

Table 1. Surface stress profile in ring compression test.

m	S <sub>E</sub>		S <sub>EV</sub> /  V <sub>Die</sub>		V <sub>S</sub> /  V <sub>Die</sub>		D <sub>S</sub> / D <sub>stroke</sub>		P / Y	
	Avg.	Max.	Avg.	Max.	Avg.	Max.	Avg.	Max.	Avg.	Max.
0.0	1.985*	1.985	0.404*	0.405	1.538*	2.025*	0.920*	1.210*	1.000	1.000
0.1	1.951	2.131	0.374	0.561	0.792	1.428	0.585	0.943	1.146	1.576
0.2	1.842	2.140*	0.285	0.585*	0.551	1.177	0.380	0.744	1.254	2.259
0.3	1.706	1.940	0.274	0.537	0.548	1.156	0.265	0.590	1.436	5.114*
0.4	1.564	1.769	0.238	0.512	0.487	1.050	0.173	0.419	1.549	4.755
0.5	1.392	1.668	0.214	0.506	0.406	0.967	0.126	0.316	1.670	4.758
0.6	1.315	1.564	0.192	0.494	0.347	0.890	0.097	0.261	1.777	4.804
0.7	1.259	1.463	0.168	0.469	0.276	0.811	0.073	0.213	1.884	4.781
0.8	1.205	1.353	0.144	0.413	0.220	0.739	0.051	0.164	1.995	4.804
0.9	1.143	1.237	0.109	0.329	0.152	0.611	0.030	0.108	2.088	4.917
1.0	1.000	1.000	0.000	0.000	0.000	0.000	0.000	0.000	2.158*	4.842

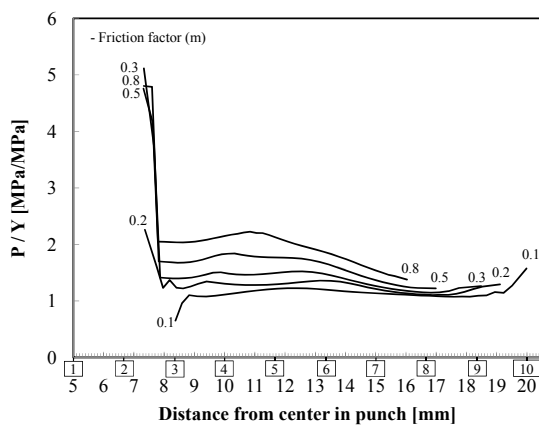


Fig. 10. Contact pressure for various friction factors.

that tool stress in terms of sliding distance increases as the distance of location of the die surface increases away from the center and this trend is amplified with decreasing friction factor. More intensive sliding movement is also seen in the figure at low friction at the regions away from the center.

Fig. 10 shows the normalized contact pressure (P/Y) distributions on the die surface. It is seen that pressure exerted on the die surface is relatively low and uniformly distributed over the whole contact surface at low friction. However, the contact pressure goes up sharply at the region near the inner periphery of the workpiece for friction factors greater than 0.3.

**4. Discussion**

The analysis results in this paper are summarized in Table 1 in terms of averaged and extreme values. It is clear from the table that the friction value at the interface is influenced much by surface expansion, contact pressure and sliding speed, and the tool wear mainly by contact pressure and sliding distance, respectively. It is interesting to note in the table that the maximum values of the surface stresses in terms of average and extreme occur at low friction, that is, for friction factor less

than 0.2, except for the contact pressure of which average and localized maximums occurs at friction factors of 1.0 and 0.3, respectively. Clearly, the ring compression test can be used efficiently to measure frictional condition at the interface only for low friction, say friction factors less than 0.2 or 0.3 which is the case for cold forming processes, and for the forming processes which are not experiencing severe deformation. The difference between averaged values over the whole contact surface and its localized maximum is relatively high such that homogeneity of the surface stress over the contact surface decreases as the friction factor increases.

**5. Conclusions**

The main results of this study in terms of stress profiles, which are in good agreement with experimental results [14], can be used as a guideline to restrict the application of the ring compression test for friction calibration curves, since friction condition at the interface would be influenced much by sliding speed, pressure, surface expansion and so on. For example, the ring compression test may not be a good method to obtain a frictional condition at the interface for backward extrusion, which is one of the most critical cold-forming processes due to very high surface expansion, extremely severe contact pressure, and relative sliding velocity between tool and workpiece which exceed 10, 10, and 6, respectively. Following conclusions can be drawn as results of this study in detail.

- (1) Contact surface generated by folding may have great influence on the dimensional changes of the ring specimen by decreasing drastically the sensitivity of conventional friction calibration curves in ring compression test at high friction greater than  $m = 0.2$ , above which the conventional friction calibration curves lose much sensitivity to friction condition due to severe folding.
- (2) Location of maximum surface expansion velocity is predicted to move outward and its peak value decreases gradually as the friction factor increases, while the difference between peak values for various friction factors is not remarkable.
- (3) Relative sliding movement gradually increases as the location of die surface increases in the radial direction. The sliding movement occurs more widely on the contact surface at low friction. Relative sliding movement in the direction of center is predicted insignificant and this trend is intensified with increasing friction factors.
- (4) Predicted tool surface stress through sliding distance increases as the distance of die surface increases away from the center and this trend is amplified with decreasing friction factor.
- (5) Pressure exerted on the die surface is predicted relatively low and uniformly distributed over the whole contact surface at low friction. However, the contact pressure goes up sharply at the region near inner periphery of workpiece for the friction factors greater than 0.3, except where more or less uniformly distributed over the whole contact area.

## Acknowledgment

This paper was published with support of Inha University Research Grant, Korea.

## References

- [1] R. B. Sims, The calculation of roll force and torque in hot rolling mills, *Proc. of the Institution of Mechanical Engineers*, London, UK 168 (1954) 191-200.
- [2] S. Kobayashi, S. I. Oh and T. Altan, *Metal Forming and The Finite Element Method*, Oxford University Press, New York, USA (1989).
- [3] A. Nadai, The force required for rolling steel strip under tension, *Journal of Applied Mechanics*, 6 (1939) A54-A69.
- [4] O. C. Zienkiewicz, P. C. Jain, and E. Onate, Flow of solids during forming and extrusion: some aspects of numerical solutions, *International Journal of Solids and Structures*, 14 (1978) 15-38.
- [5] D. V. Tran, R. W. Lewis, D. T. Gethin and A. K. Afriffin, Numerical modeling of powder compaction processes: displacement based finite element method, *Powder Metallurgy*, 36 (1993) 257-166.
- [6] G. J. Li and S. Kobayashi, Rigid plastic finite element analysis of plane strain rolling, *Journal of Engineering for Industry-Transactions of the ASME*, 104 (1982) 55-64.
- [7] J. R. Cho, C. Y. Park and D. Y. Yang, Investigation of the cogging processes by three-dimensional thermo-viscoplastic finite element analysis, *Proc. of the Institution of Mechanical Engineers*, 206 (1992) 277-286.
- [8] J. J. Park and S. I. Oh, Application of three dimensional finite element analysis of shape rolling processes, *Journal of Engineering for Industry-Transactions of the ASME*, 112 (1990) 34-46.
- [9] T. Coupez, N. Soyris and J. L. Chenot, 3-d finite element modeling of the forging process with automatic remeshing, *Journal of Materials Processing Technology*, 27 (1991) 119-133.
- [10] M. S. Joun, H. G. Moon, I. S. Choi, M. C. Lee and B. Y. Jun, Effects of friction laws on metal forming processes, *Tribology International*, 42 (2009) 311-319.
- [11] T. Robinson, H. Ou and C. G. Armstrong, Study on ring compression test using physical modeling and FE simulation, *Journal of Materials Processing Technology*, 153-154 (2004) 54-49.
- [12] SFTC, *DEFORM-2D Ver. 8.0 Users Manual*, Scientific Forming Technologies Corporation Inc., New York, USA (2004).
- [13] C. H. Lee and S. Kobayashi, New solutions to rigid-plastic deformation problems using a matrix method, *Journal of Engineering for Industry-Transactions of the ASME*, 95 (1973) 865-873.
- [14] K. Lange and Th. Gräbener, *Tribologische aspekte bei den verfahren der umformtechnik*, Technische Akademie Esslingen, Oktober, Germany (1980).



**Beong Bok Hwang** received his B.S. in Mechanical Engineering from Inha University, Incheon, Korea, in 1981. He received his M.S. and then Ph.D. degrees from Univ. of Michigan, Ann Arbor and U.C. Berkeley in 1985 and 1991, respectively. Dr. Hwang is currently a Professor at the School of Mechanical Engineering at Inha University in Incheon, Korea. Dr. Hwang's research interests include metal forming process.



**Jeong Hoon Noh** received his B.S. in Mechanical Engineering from Inha University, Incheon, Korea, in 2008. He received his M.E. from Inha University in 2010. Mr. Noh is currently a Ph.D. candidate at the Department of Mechanical Engineering at Inha University in Incheon, Korea.



**Min Tae Kim** received his B.S. in Mechanical Engineering from Wonkwang University, Iksan, Korea, in 2008. He received his M.E. from Inha University in 2010.